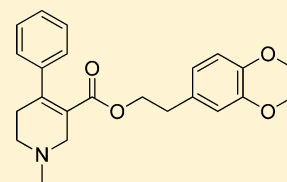


Structural Modifications to Tetrahydropyridine-3-carboxylate Esters en Route to the Discovery of M₅-Preferring Muscarinic Receptor Orthosteric AntagonistsGuangrong Zheng,^{*,†} Andrew M. Smith,[‡] Xiaoqin Huang,[‡] Karunai L. Subramanian,[‡] Kiran B. Siripurapu,[‡] Agripina Deaciuc,[‡] Chang-Guo Zhan,[‡] and Linda P. Dwoskin[‡][†]Department of Pharmaceutical Sciences, College of Pharmacy, University of Arkansas for Medical Sciences, Little Rock, Arkansas 72205, United States[‡]Department of Pharmaceutical Sciences, College of Pharmacy, University of Kentucky, Lexington, Kentucky 40536, United States

S Supporting Information

ABSTRACT: The M₅ muscarinic acetylcholine receptor is suggested to be a potential pharmacotherapeutic target for the treatment of drug abuse. We describe herein the discovery of a series of M₅-preferring orthosteric antagonists based on the scaffold of 1,2,5,6-tetrahydropyridine-3-carboxylic acid. Compound **56**, the most selective compound in this series, possesses an 11-fold selectivity for the M₅ over M₁ receptor and shows little activity at M₂–M₄. This compound, although exhibiting modest affinity ($K_i = 2.24 \mu\text{M}$) for the [³H]N-methylscopolamine binding site on the M₅ receptor, is potent ($\text{IC}_{50} = 0.45 \text{ nM}$) in inhibiting oxotremorine-evoked [³H]DA release from rat striatal slices. Further, a homology model of human M₅ receptor based on the crystal structure of the rat M₃ receptor was constructed, and docking studies of compounds **28** and **56** were performed in an attempt to understand the possible binding mode of these novel analogues to the receptor.



■ INTRODUCTION

Muscarinic acetylcholine receptors (mAChRs) are G-protein-coupled receptors (GPCRs) activated by the endogenous neurotransmitter acetylcholine (ACh) and the natural alkaloid muscarine. Upon ACh activation, these receptors regulate a variety of central and peripheral physiological functions such as cognition, movement, sleep, cardiovascular function, smooth-muscle contractility, and glandular secretion.^{1–4} Thus, mAChRs have emerged as important therapeutic targets for many diseases, such as Alzheimer's disease, Parkinson's disease, psychosis, pain, asthma, diabetes, and smooth-muscle disorders.^{3,4} Five mAChR subtypes (M₁–M₅) have been identified.² Each of the five mAChR subtypes has a defined distribution pattern within specific brain regions and peripheral tissues and mediates distinct physiological functions.^{1–4} To avoid side effects, selectivity at specific mAChR subtypes is often a major focus of discovery of mAChR agonists and antagonists as therapeutic agents.

The M₅ mAChR was the last subtype to be cloned.^{2,5} A growing body of evidence suggests that this subtype is a potential target for the discovery of treatments for drug abuse.⁶ The rewarding effects of abused drugs are believed to be mediated by the mesolimbic dopamine (DA) pathway, which projects from the midbrain ventral tegmental area (VTA) to the nucleus accumbens.^{7–10} M₅ mAChRs are the only muscarinic subtype localized to VTA and that modulate DA release from VTA DA neurons.^{11–17} Consistent with M₅ mAChR modulation of mesolimbic DA transmission, behavioral studies using M₅ knockout mice show a reduction in reward and withdrawal responses following repeated morphine or cocaine administration, as well as a reduction in the rate of cocaine self-administration.^{18–21}

Furthermore, microinfusion into VTA of an antisense oligonucleotide targeting M₅ receptor mRNA inhibits brain stimulation reward in rats¹⁵ and microinfusion into the VTA of the nonselective mAChR antagonist, scopolamine (**1**, Figure 1), reduces cocaine-facilitated DA release in nucleus accumbens.¹⁷ Microinfusion of the nonselective mAChR antagonist atropine (**2**, Figure 1) into the VTA in rats dose-dependently inhibits morphine-induced conditioned place preference.²² Taken together, these studies suggest that discovery of subtype-selective M₅ mAChR antagonists may provide novel treatments for drug abuse. Importantly, mice lacking M₅ receptors exhibit no difference from their wild-type littermates in various behavioral and pharmacologic tests,^{18,23} suggesting that centrally active M₅ receptor antagonists will be well tolerated.

Subtype-selective M₅ receptor antagonists also will be useful pharmacological tools in defining the physiological functions of this receptor. Currently, little information is available on the effects of selective activation or inhibition of M₅ receptors. Recent success in identifying M₅-selective positive allosteric modulators may provide new information in this regard.^{24–26} Nevertheless, no subtype-selective orthosteric M₅ antagonists are available to date. Unlike allosteric binding sites, which are usually more divergent across subtypes, orthosteric ACh binding sites across the five mAChR subtypes have been shown to be highly conserved at the amino acid sequence level (73–83% identity).⁵ As such, selectivity among the mAChR subtypes is likely based on conformational dissimilarities rather than upon

Received: November 21, 2012

Published: February 4, 2013

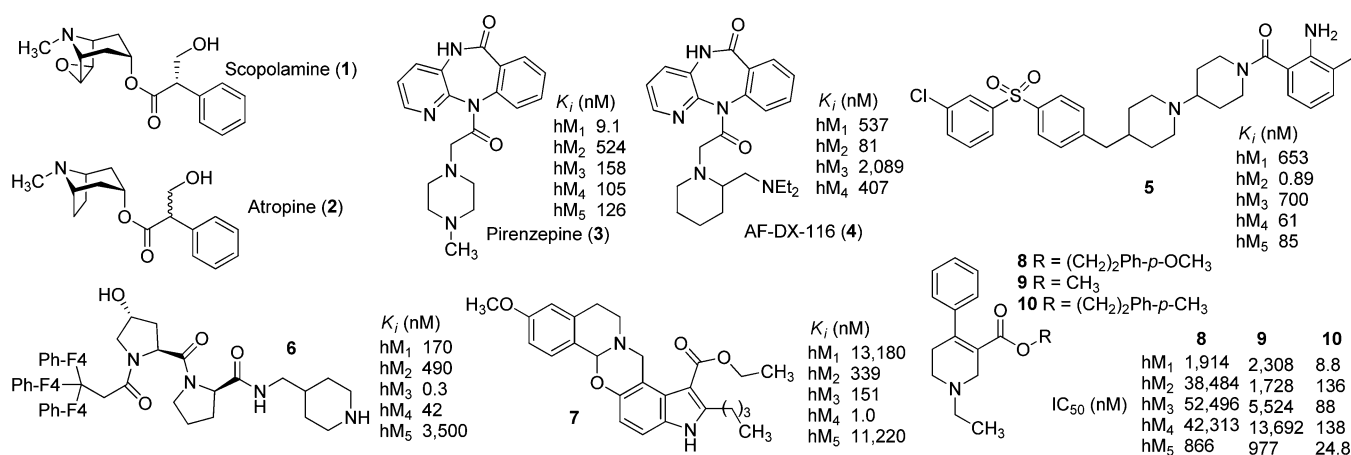


Figure 1. Structures of selected mAChR antagonists and their literature reported mAChR affinity data.

single amino acid residues.^{27–29} In fact, small molecule orthosteric antagonists with preference for an individual subtype have been reported for M₁–M₄ but not M₅ (e.g., compound 3 for M₁,³⁰ 5 for M₂,³¹ 6 for M₃,³² and 7 for M₄,²⁹ Figure 1), indicating the existence of sufficient differences among the agonist recognition sites on the five mAChR subtypes allowing targeting of selective compounds to these sites.

Radioligand binding assays using membranes from recombinant cells expressing human mAChRs (hM₁–hM₅) show that compound 8 (1-ethyl-4-phenyl-1,2,5,6-tetrahydropyridine-3-carboxylic acid 4-methoxyphenethyl ester, Figure 1) preferentially binds to the M₅ receptor (subtype selectivity: M₁/M₅ = 2.2-fold, M₂/M₅ = 44-fold, M₃/M₅ = 60-fold, M₄/M₅ = 48-fold, Figure 1).³³ Thus, the current exploration of the structure–activity relationship (SAR) regarding M₅ selective orthosteric ligands is based on compound 8. To our best knowledge, compound 8 and its analogue 9 (Figure 1) are the only orthosteric small molecules reported to exhibit preference for M₅ receptors.³³

The current structural modification strategy is provided in Figure 2. The 1,2,5,6-tetrahydropyridine-3-carboxylate core structure

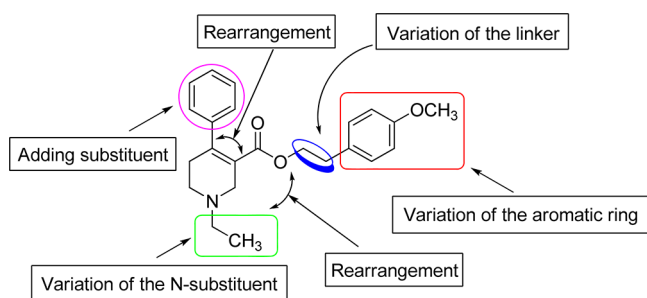


Figure 2. General structural modification strategy.

was retained while modifying each part of the “appending” pharmacophores in a stepwise manner. These “appending” pharmacophores were to be rearranged around the core structure in compound 8 (Figure 2). Herein, we report the synthesis, pharmacological evaluation, and SAR analysis of this new series of mAChR antagonists. Additionally, a homology model of hM₅ mAChR was constructed based on the crystal structure of the rat M₃ mAChR. Preliminary docking experiments were performed using this model in an attempt to understand the structural basis of the interaction between these ligands and the receptor.

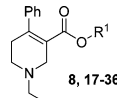
RESULTS AND DISCUSSION

Synthesis. The general synthetic methods for analogues 17–36 (Table 1) with modifications on the *p*-methoxyphenethyl moiety of compound 8 are depicted in Scheme 1. Transformation of commercially available ethyl 1-benzyl-4-oxo-3-piperidinecarboxylate (11) into compound 12 was achieved by initial conversion of 11 to *N*-BOC protected compound via a two-step process,³⁴ followed by triflation under diisopropylamine and trifluoromethanesulfonic anhydride.³⁵ Suzuki coupling of 12 with phenylboronic acid afforded compound 13. Removal of BOC in 13 by TFA afforded compound 14, which was then *N*-ethylated to form compound 15. Compound 15 was subjected to ester hydrolysis under basic conditions to afford carboxylic acid 16. Treatment of 16 under a Steglich esterification condition with appropriate alcohols afforded 8 and its analogues 17–36. The synthetic route for analogues with variations on the *N*-ethyl moiety of compound 8 was initially devised to introduce the *N*-substituent at the last step. Accordingly, compound 13 was converted to compound 38 in a sequence similar to that for compound 15 to 8 (Scheme 1). However, deprotection of 38 to form 39 using various de-BOC methods (TFA/CH₂Cl₂, HCl/EtOAc, AcCl/MeOH, or TsOH/CH₂Cl₂) resulted in complex mixtures. Attempts to purify compound 39 by silica gel column chromatography failed. Impure intermediate 39 (obtained from TFA treatment) was employed to provide *N*-Me, *N*-*n*-Pr, *N*-*n*-Bu, or *N*-*p*-methoxybenzyl analogues via reductive amination, but only *N*-*p*-methoxybenzyl analogue (compound 40) was obtained in pure form after preparative TLC purification. Alternatively, a similar route to that for analogues 17–36 was applied to prepare analogues 42–59 from compound 14 (Scheme 1, Table 2).

Analogues 61–69 (Table 2) were synthesized in a similar manner to analogues 42–59 from triflate 12. Phenyl ring substituted phenylboronic acids were used instead of phenylboronic acid as the Suzuki coupling partners (Scheme 2).

Analogues 70–73 were prepared by *N*-alkylation of compound 14 with appropriate alkyl halides (Scheme 3). Analogues 74–76 were prepared by reductive amination of compound 14 with an *N*-sulfonated or *N*-acylated 4-piperidinone using sodium triacetoxyborohydride (Scheme 3).

The syntheses of analogues 84 and 85 were initially attempted by applying a route similar to that used for the synthesis of their regioisomers in Scheme 1 (analogues 56 and 45, respectively), starting from ethyl 1-benzyl-3-oxo-4-piperidinecarboxylate hydrochloride (77) (Scheme 4). However, de-BOC reaction of

Table 1. Structures and Binding Affinity for Scopolamine (1), 8, and 17–36 at the hM₁ and hM₅ mAChRs^a


compd	R ¹	K _i , nM		
		hM ₁	hM ₅	hM ₁ /hM ₅
1	-	7.5	17.6	0.4
8		170	420	0.4
17		1,730	1,250	1.4
18		470	150	3.1
19		3,060	3,610	0.8
20		3,290	470	7.0
21		>100,000	>100,000	-
22		200	290	0.7
23		100	190	0.5
24		560	410	1.4
25		240	370	0.6
26		810	440	1.8
27		>100,000	>100,000	-
28		1,390	230	6.0
29		200	280	0.7
30		60	120	0.5
31		11,700	2,460	4.8
32		>100,000	>100,000	-
33		>100,000	>100,000	-
34		410	760	0.5
35		370	140	2.6
36		140	190	0.7

^aAt least three independent experiments with samples evaluated in duplicate were performed to obtain the K_i value.

compound 78 failed to yield the desired intermediate 79. As an alternative, analogues 84 and 85 were synthesized starting from 3-bromoisonicotinic acid (80). Ethyl esterification of 80 followed by Suzuki coupling with phenylboronic acid afforded

compound 81, which was treated with methyl iodide to yield the corresponding quaternary pyridinium salt 82. Reduction of 82 with sodium borohydride gave 1,2,5,6-tetrahydropyridine derivative 83, which underwent ester hydrolysis and subsequent esterification with appropriate alcohols to afford analogues 84 and 85.

Synthesis of analogue 89 was achieved by initial Suzuki coupling of 4-bromopyridine with 2-(ethoxycarbonyl)phenylboronic acid, followed by a route similar to that for analogues 84 and 85 from compound 81 (Scheme 5).

Radioligand Binding Assay. Receptor affinities were determined by measuring inhibition of the binding of [³H]N-methylscopolamine (NMS), an orthosteric antagonist probe, to membranes from Chinese hamster ovary (CHO) cells individually expressing human hM₁–hM₅ mAChR receptors. Compound 1 (scopolamine) and compound 8 were used as reference compounds. Methods for these binding assays are described briefly in the Experimental Section. All synthesized analogues were evaluated first at hM₁ and hM₅ subtypes (Table 1 and 2, Scheme 3–5). Selectivity for M₅ over M₁ is important because antagonism of CNS M₁ receptors has been suggested to result in cognitive deficits³⁶ and to increase DA release in striatum.³⁷ Binding affinity for analogues that exhibited binding preference for M₅ over M₁ was determined at each of the five mAChR subtypes (Table 3).

Identification of compound 8 was the starting point. Compound 8 was an analogue of the 1-ethyl-4-phenyltetrahydropyridine-3-carboxylic acid scaffold aimed at identifying M₁ selective antagonists. Compound 8 was reported to have a 2.2-fold preference for M₅ over M₁ and to be more than 40-fold selective for M₅ over M₂–M₄ mAChR subtypes (Figure 1).³³ However, in the current study, compound 8 showed no selectivity for M₅ over M₁–M₄ (Table 3). Preliminary SAR from the previous report³³ suggested that small changes on the *p*-methoxyphenyl ring of 8 afforded remarkably different binding affinity and selectivity profiles at mAChR subtypes. For example, when the methoxy group on the phenyl ring of 8 was replaced by a methyl group, the resulting analogue 10 bound preferentially to the M₁ receptor, while binding affinity at the M₅ receptor increased 35-fold, when compared to compound 8 (Figure 1).³³

Results in Table 1 summarize the modifications to the *p*-methoxyphenethyl moiety of compound 8 evaluated in the current study and the influence of these modifications on binding affinity and selectivity for M₁ and M₅ receptors. Results from para-, meta-, and ortho-methoxy analogues 8, 17, and 18, respectively, indicate that the meta-substitution was favorable to M₅ selectivity. Compared to 8 (K_i = 420 nM) and 17 (K_i = 1250 nM), meta-analogue (18, K_i = 150 nM) exhibited a small 3- and 8-fold, respectively, increase in affinity at M₅ over M₁. Replacement of the ethylene link in the *p*-methoxyphenethyl moiety by a methylene (compound 19, K_i = 3610 nM) or a methylethylene link (compound 21, K_i > 100 μM) significantly decreased binding potency at M₅ receptor, whereas replacement with a propylene link (compound 20, K_i = 470 nM) retained binding affinity at M₅ and markedly increased selectivity (7-fold) over M₁ receptors. Interestingly, there were no marked differences in M₅ affinities when the 4-methoxy was replaced with another para-substitution group, including halogens (compounds 23–25) and nitro group (compound 26), indicating modification at this position is somewhat tolerated. However, compound 27, in which a 4-methylsulfonyl group was attached to the phenyl ring, exhibited little affinity for either M₁ or M₅ receptors. Compounds 28 and 31, wherein both 3- and 4-positions of the phenyl ring were substituted, not

Chemical reaction scheme showing the synthesis of 2-phenyl-1,2,3,4,5,6-hexahydropyridine-3-carboxylic acid derivatives (8, 17-36) from compound 11.

Starting material: 11 (2-phenyl-1,2,3,4,5,6-hexahydropyridine-3-carboxylic acid ethyl ester hydrochloride).

Reagents and conditions:

- a, b, c: 11 → 12 (2-phenyl-1,2,3,4,5,6-hexahydropyridine-3-carboxylic acid ethyl ester, Boc-protected)
- d: 12 → 13 (2-phenyl-1,2,3,4,5,6-hexahydropyridine-3-carboxylic acid ethyl ester, Boc-protected)
- e: 13 → 14 (2-phenyl-1,2,3,4,5,6-hexahydropyridine-3-carboxylic acid ethyl ester, Boc-protected)
- f: 14 → 15 (2-phenyl-1,2,3,4,5,6-hexahydropyridine-3-carboxylic acid ethyl ester, Boc-protected)
- g: 15 → 16 (2-phenyl-1,2,3,4,5,6-hexahydropyridine-3-carboxylic acid, Boc-protected)
- h: 16 → 38 (2-phenyl-1,2,3,4,5,6-hexahydropyridine-3-carboxylic acid, Boc-protected)
- e: 38 → 39 (2-phenyl-1,2,3,4,5,6-hexahydropyridine-3-carboxylic acid, Boc-protected)
- i: 39 → 40 (2-phenyl-1,2,3,4,5,6-hexahydropyridine-3-carboxylic acid, Boc-protected)
- g: 13 → 37 (2-phenyl-1,2,3,4,5,6-hexahydropyridine-3-carboxylic acid, Boc-protected)
- j: 14 → 41 (2-phenyl-1,2,3,4,5,6-hexahydropyridine-3-carboxylic acid ethyl ester, Boc-protected)
- g, h or k: 41 → 42-59 (2-phenyl-1,2,3,4,5,6-hexahydropyridine-3-carboxylic acid ethyl ester, Boc-protected)
- h: 16 → 8, 17-36 (2-phenyl-1,2,3,4,5,6-hexahydropyridine-3-carboxylic acid, Boc-protected)

Structure 40 is shown with R² = *p*-methoxybenzyl.

Second, the ester group on C3 and the phenyl group on C4 of the 1,2,5,6-tetrahydropyridine ring in compounds **56** and **45** were transposed to produce compounds **84** and **85** (Scheme 4), respectively. Both compounds **84** ($M_1/M_5 = 2.4$) and **85** ($M_1/M_5 = 2.1$) displayed reduced selectivity for M_5 over M_1

Table 2. Structures and Binding Affinity for Analogues 40, 42–59, and 61–69 at the hM₁ and hM₅ mAChRs^a

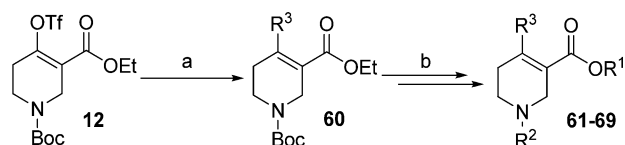
40, 42–59, 61–69

compd	R ¹	R ²	R ³	K _i , nM		hM ₁ /hM ₅
				hM ₁	hM ₅	
40		4-MeO-Bn	Ph	>100,000	>100,000	-
42	<i>ibid.</i>	Me	Ph	20	30	0.7
43	<i>ibid.</i>	<i>n</i> Pr	Ph	>100,000	>100,000	-
44	<i>ibid.</i>	<i>n</i> Bu	Ph	>100,000	>100,000	-
45		Me	Ph	290	60	4.8
46	<i>ibid.</i>	<i>n</i> Pr	Ph	>100,000	>100,000	-
47	<i>ibid.</i>	<i>n</i> Bu	Ph	>100,000	>100,000	-
48		Me	Ph	5,400	1,160	4.7
49		Me	Ph	>100,000	>100,000	-
50		Me	Ph	920	630	1.5
51		Me	Ph	340	190	1.8
52		Me	Ph	510	110	4.6
53		Me	Ph	880	280	3.1
54		Me	Ph	330	80	4.1
55		Me	Ph	2,700	740	3.6
56		Me	Ph	25,300	2,240	11.3
57		Me	Ph	24,400	5,040	4.8
58		Me	Ph	>100,000	>100,000	-
59		Me	Ph	6,190	3,070	2.0
61		Et	4-F-Ph	7,900	2,350	3.4
62	<i>ibid.</i>	Me	3-F-Ph	>100,000	>100,000	-
63	<i>ibid.</i>	Me	2-F-Ph	5,270	740	7.0
64	<i>ibid.</i>	Me	3-MeO-Ph	2,430	2,680	0.9
65	<i>ibid.</i>	Me	2-MeO-Ph	8,350	2,410	3.5
66		Me	3-F-Ph	27,000	3,340	8.1
67	<i>ibid.</i>	Me	2-F-Ph	>100,000	>100,000	-
68	<i>ibid.</i>	Me	3-MeO-Ph	>100,000	>100,000	-
69	<i>ibid.</i>	Me	2-MeO-Ph	>100,000	>100,000	-

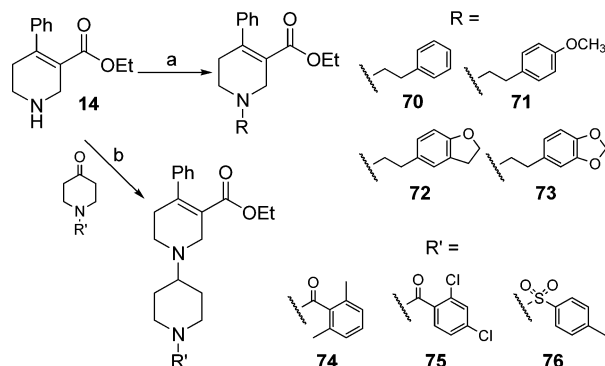
^aAt least three independent experiments with samples evaluated in duplicate were performed to obtain the K_i value.

receptors when compared to their corresponding position isomers, 56 and 45, respectively. Last, the ester functionality in compound 45 was moved from C3 of the tetrahydropyridine ring to the

phenyl ring on C4 (compound 89, Scheme 5). This “parallel” shift resulted in a complete loss of binding affinity at both M₁ and M₅ receptors.

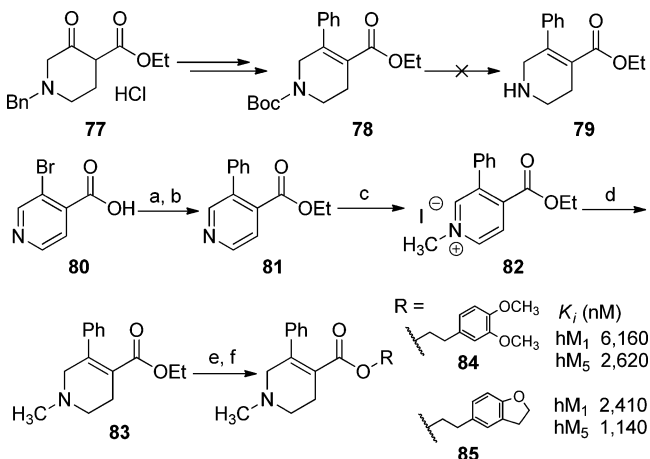
Scheme 2. Synthesis of Compounds 61–69^a

^aReagents and conditions: (a) substituted phenylboronic acids, Pd(PPh₄)₃, Na₂CO₃ (2.0 M), THF, 65 °C; (b) same as from compound 13 to 42 in Scheme 1.

Scheme 3. Synthesis of Compounds 70–76^a

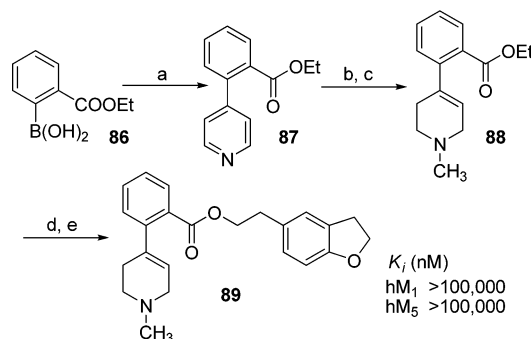
70–76, not active at hM₁ and hM₅ ($K_i > 100,000$ nM)

^aReagents and conditions: (a) alkyl bromides, KI, K₂CO₃, CH₃CN, reflux; (b) NaBH(OAc)₃, HOAc, THF, 65 °C for 74, rt for 75 and 76.

Scheme 4. Synthesis of Compounds 84 and 85^a

^aReagents and conditions: (a) EtOH, H₂SO₄ (conc), reflux; (b) PhB(OH)₂, Pd(PPh₄)₃, Na₂CO₃ (2.0 M), THF, 65 °C; (c) MeI, acetone; (d) NaBH₄, EtOH; (e) 10% KOH (H₂O)/EtOH (1:1); (f) alcohols, EDCI, DMAP, CH₂Cl₂.

At saturation concentrations, all analogues except for those with $K_i > 100,000$ nM exhibited complete inhibition (maximal inhibition $I_{\max} = 100\%$, data not shown) of the binding of the orthosteric antagonist [³H]NMS at mAChRs, which is consistent with an orthosteric mechanism of action. Selected compounds, including 20, 28, 45, 56, 57, 63, and 66, that exhibited binding preference for hM₅ over hM₁ mAChRs were also evaluated for affinity at M₂, M₃, and M₄ mAChR subtypes (Table 3). Results showed that five of these seven compounds exhibited good selectivity for M₅ over M₂, M₃, and M₄ receptors. The most selective compound, 56 (11-fold for M₅

Scheme 5. Synthesis of Compound 89^a

^aReagents and conditions: (a) 4-bromopyridine, Pd(PPh₃)₄, Na₂CO₃ (2.0 M), THF, 65 °C; (b) MeI, acetone; (c) NaBH₄, EtOH; (d) 10% KOH (H₂O)/EtOH (1:1); (e) 2-(2,3-dihydrobenzofuran-5-yl)-ethanol, EDCI, DMAP, CH₂Cl₂.

over M₁ receptor), had no affinity ($K_i > 100 \mu\text{M}$) at the M₂, M₃, and M₄ mAChR subtypes. Compound 28 exhibited 6-fold, >435-fold, 135-fold, and 46-fold for M₅ over M₁, M₂, M₃, and M₄, respectively. Although slightly less selective for the M₅ over the M₁ receptor, it exhibited higher affinity at M₅ when compared to compound 56.

Inhibition of Oxotremorine-Evoked Striatal [³H]DA Release. In vitro functional assays for mAChR antagonists measure the ability of molecules to block mAChR agonist-induced receptor activation at recombinant mAChR subtypes expressed in cells.⁴¹ Pharmacological studies of M₅ receptors using mouse basilar artery have also been reported.⁴² However, these recombinant and native M₅ receptors functional assays are far removed from a potential role for M₅ receptors in cocaine and opiate addiction. Studies have shown that oxotremorine, a non-selective mAChR agonist, concentration-dependently increases [³H]DA release from striatal slices prepared from wild-type mice and that oxotremorine-evoked striatal [³H]DA release was reduced significantly in M₅ receptor knockout mice.^{18,43} We hypothesized that an M₅ receptor selective antagonist would also reduce oxotremorine-mediated rat striatal [³H]DA release. Current results show that oxotremorine evokes [³H]DA release from rat striatal slices and that scopolamine inhibits this effect in a concentration-dependent manner (Figure 4). These results support the contention that this functional assay probes native M₅ receptors. Furthermore, this functional assay is highly relevant to the underlying dopaminergic mechanisms involved in drug reward and abuse.

Results revealed that compound 56 inhibited ($IC_{50} = 0.45$ nM) oxotremorine (100 μM) evoked [³H]DA release from rat striatal slices (Figure 5). Unlike scopolamine (1 μM), which completely inhibits oxotremorine-mediated [³H]DA release from rat striatal slices (Figure 4), compound 56 produced maximal inhibition (I_{\max}) of only 48% of the oxotremorine-evoked [³H]DA release (Figure 5). These current results are consistent with previous reports that ~50% of oxotremorine-evoked [³H]DA release from striatal slices was eliminated in M₅ knockout mice compared to wild-type mice,¹⁸ indicating that other mAChR subtype(s) also mediate oxotremorine-evoked striatal DA release. In agreement with this hypothesis, studies using mAChR knockout mice suggested that M₃ and M₄ receptors were also involved in mediating striatal DA release.⁴³ The observations that both compound 56 and the deletion of the M₅ receptor resulted in similar effects on oxotremorine-evoked striatal [³H]DA release, together with the

Table 3. Binding Affinity and Selectivity for Selected Analogues at the hM₁–hM₅ mAChRs^a

compd	K _i , nM				
	hM ₅	hM ₁ (M ₁ /M ₅) ^b	hM ₂ (M ₂ /M ₅) ^b	hM ₃ (M ₃ /M ₅) ^b	hM ₄ (M ₄ /M ₅) ^b
1	17.6	7.5 (0.4)	9.5 (0.5)	6.5 (0.4)	36.9 (2.1)
8	420	170 (0.4)	1100 (2.6)	1370 (3.3)	1730 (4.1)
20	470	3290 (7.0)	2030 (4.3)	4070 (8.7)	11500 (24)
28	230	1390 (6.0)	>100000 (>435)	31100 (135)	10500 (46)
45	60	290 (4.8)	1170 (20)	2840 (47)	1890 (32)
56	2240	25300 (11)	>100000 (>45)	>100000 (>45)	>100000 (>45)
57	5040	24400 (4.8)	>100000 (>20)	>100000 (>20)	>100000 (>20)
63	740	5270 (7.1)	540 (0.7)	4890 (6.6)	5740 (7.8)
66	3340	27000 (8.0)	>100000 (>30)	>100000 (>30)	>100000 (>30)

^aAt least three independent experiments with samples evaluated in duplicate were performed to obtain the K_i value. ^bNumbers in the parentheses are the ratios of binding affinity between M₅ and the respective subtype.

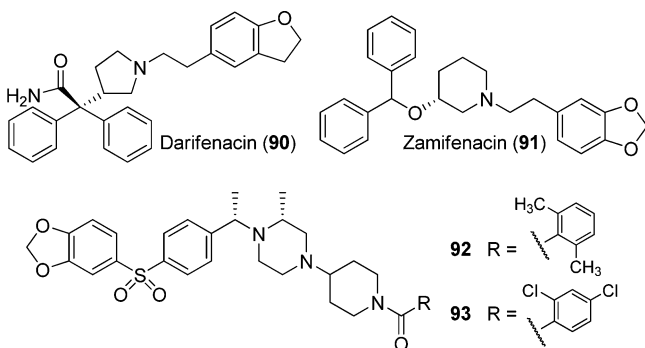
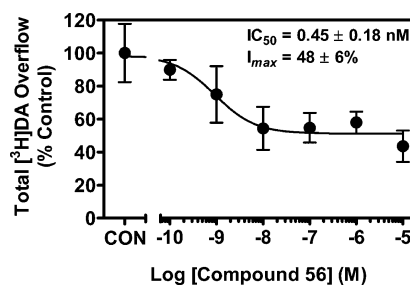


Figure 3. Structures of darifenacin (90), zamifenacin (91), and compounds 92 and 93.

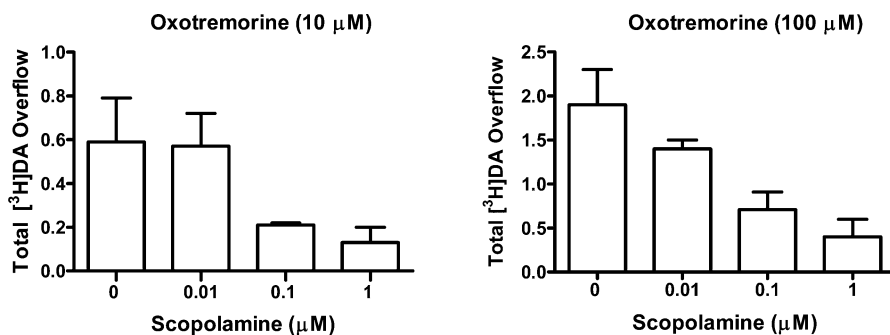
selective binding of **56** to M₅ over M₃ and M₄ receptors, strongly suggest that **56** interacts with M₅ receptors to inhibit muscarinic agonist-induced striatal DA release.

It is noteworthy that compound **56** (IC₅₀ = 0.45 nM) appears more potent than scopolamine in inhibiting oxotremorine-evoked [³H]DA release from rat striatal slices, although its [³H]NMS binding affinity on the M₅ receptor is 127-fold less than scopolamine. One explanation of the lack of correlation between binding and function is that the [³H]NMS binding assay was performed on a single receptor in a recombinant system but the [³H]DA release assay was on heterogeneous brain slices. Compound **56** may potentially act at other sites that also inhibit [³H]DA release. Alternatively, recent studies on the crystal structure of the rat M₃ receptor with antagonist tiotropium bound to the orthosteric binding site suggested that tiotropium binds transiently to an allosteric site en route to the

Figure 5. Compound **56** inhibits oxotremorine (100 μM) evoked [³H]DA release from rat striatal slices (data are expressed as the mean ± SEM, n = 4).

orthosteric binding pocket.⁴⁴ Compound **56** could have a similar allosteric interaction with the receptor, causing the inhibition of oxotremorine-evoked striatal [³H]DA release. However, further pharmacological studies are needed to elucidate the mechanism.

Binding Mode for M₅ mAChRs for Lead Compounds 28 and 56. To study the interaction of our compounds with M₅ mAChR in atomic detail, homology modeling and molecular docking operations were performed. Compounds **28** and **56** were selected for these studies, since both analogues preferentially bind to M₅ mAChR and thus can be considered current lead compounds. Importantly, compounds **28** and **56** have an order of magnitude difference in binding affinities at M₅ receptor (K_i of 230 nM vs 2240 nM, respectively). This moderate difference in affinity between **28** and **56** is ideal for testing the reliability of our homology models. The structural model of the human M₅ mAChR was constructed based on

Figure 4. Scopolamine (0.01–1 μM) inhibits oxotremorine (10 and 100 μM) evoked [³H]DA release from rat striatal slices (data are expressed as the mean ± SEM, n = 3).

the newly available X-ray crystal structure of the rat M_3 mAChR with antagonist tiotropium bound to the orthosteric binding site.⁴⁴ Compounds **28** and **56** were docked into possible binding sites among the transmembrane (TM) helices of the M_5 mAChR. Binding structures were selected from the docking results and subjected to energy minimization. In accordance with the minimized binding structures, the binding site for compounds **28** and **56** at the M_5 mAChR is the orthosteric site located near the extracellular end of TM3, TM5, TM6, and TM7. As shown in Figure 6, TM2 and TM4 are also

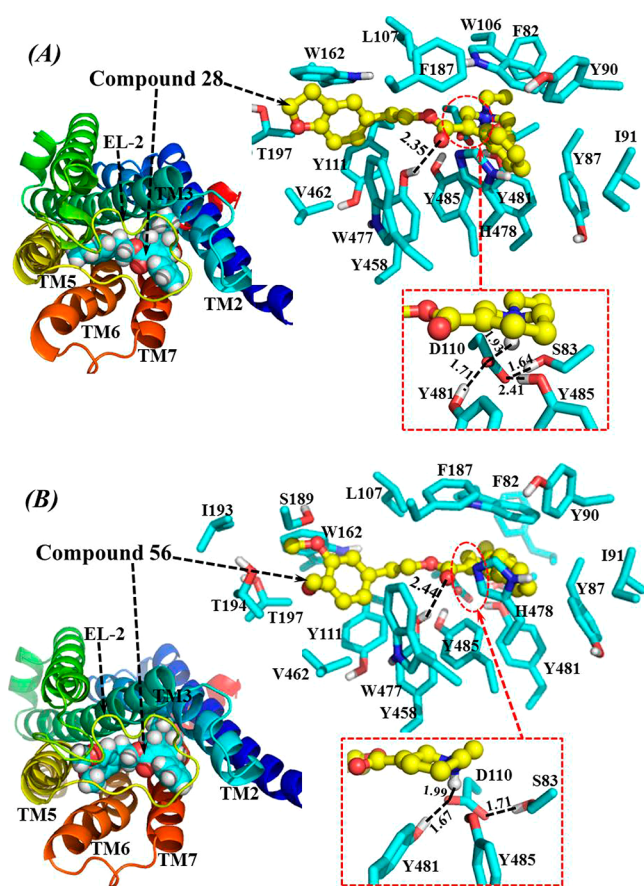


Figure 6. Homology model of human M_5 mAChR based on the X-ray crystal structure of rat M_3 mAChR (PDB entry of 4DAJ at 3.4 Å resolution, A chain). (A) Top view of the energy-minimized binding structure of M_5 mAChR–**28** complex. (B) Top view on the energy-minimized binding structure of M_5 mAChR–**56** complex. The receptor proteins in (A) and (B) are represented as ribbons in rainbow color, and compounds **28** and **56** are shown as spheres (left panel) or ball-and-stick (right panel). Residues within 5 Å of compound **28** and **56** are labeled and shown as sticks. **28** and **56** have very similar hydrogen bonding interactions with the protein, including interactions between the D110 side chain and the cationic heads of the compounds, interactions between the carbonyl oxygen atoms of the compounds and the Y458 side chain, and the interactions among side chains of D110, S83, Y481, and Y485. These hydrogen bonding interactions are shown as dashed lines along with the labeled distances.

partially involved in the formation of the antagonist-binding site. In addition, the antagonist-binding site is partially covered by extracellular loop 2 (EL-2). As depicted in Figure 6A, compound **28** is orientated horizontally inside the binding pocket. The cationic head of compound **28** is anchored around the negatively charged side chain of residue D110 of TM3, interacting

through electrostatic attraction and strong hydrogen bonding. Meanwhile, residue D110 is also hydrogen-bonded with the side chain of S83 from TM2 and with the side chains of Y481 and Y485 from TM7. The cationic head of compound **28** is in close contact with residues W106 and L107 from TM3. The phenyl group on C4 of the tetrahydropyridine ring is closely packed with Y87, Y90, and I91 from TM2, with W106 from TM3, with F187 from EL-2, and with H478 from TM7. The ethyl group at the cationic head of compound **28** makes contact with the aromatic side chain of residue F82 from TM2. The carbonyl oxygen of compound **28** is weakly hydrogen-bonded with the hydroxyl group at the side chain of Y458 from TM6. The tail group (2,3-dihydrobenzofuran-5-ethyl) of compound **28** is packed in parallel with the underneath Y111 from TM3 and packed perpendicularly with the side chain of W162 from TM4. The tail group of compound **28** is also surrounded by T197 from TM5 and by V462 from TM6.

As depicted in Figure 6B, the binding mode of the M_5 mAChR with compound **56** is essentially the same as that with compound **28**. One difference between the binding of **56** and **28** to the M_5 mAChR is that residues I193 and T194 from TM5 are both within 5 Å of compound **56** (Figure 6B), while these two residues have no contacts with compound **28** (Figure 6A). Another difference is the distance of hydrogen bonding formed by the side chain of residue D110 with the cationic headgroup of the antagonist. As shown in Figure 6, the distance between the hydrogen bonding between residue D110 and the cationic head of compound **28** is shorter than that of the hydrogen bonding between residue D110 and the cationic head of compound **56** (1.93 Å vs 1.99 Å, respectively), indicating a stronger bond with **28** than with **56** to the protein. These structural differences, especially the difference in hydrogen bonding distance, may contribute to the difference in binding affinity as represented by the experimentally measured values of K_i (230 nM for **28** vs 2240 nM for **56**) for these two lead compounds (Table 3). The modeled binding structures helped to qualitatively understand the observed SAR and provided clues to design a valuable virtual library of new analogues for computational screening.

SUMMARY

Starting from compound **8** as a lead structure, we have identified the first M_5 -preferring antagonists through a systematic structural modification strategy. The greatest mAChR selectivity and potency shifts came from the modification of the substituents on the ester group. Replacing the *N*-Et group on the tetrahydropyridine ring with an *N*-Me group generally resulted in a significant increase in mAChR binding affinity while maintaining mAChR subtype-selectivity profile. This preliminary SAR study provides a basis for further discovery of potent and selective M_5 ligands. In addition, we have successfully established a functional assay for M_5 receptors using oxotremorine-evoked DA release from superfused rat striatal slices. One of our lead compounds, **56**, demonstrated inhibition of oxotremorine-mediated striatal [3 H]DA release, with a maximal inhibition of ~50%. This result is similar to the effects of M_5 knockout on striatal [3 H]DA release, providing validation for the current assay. Further, we have constructed a homology model of human M_5 based on the newly available crystal structure of the rat M_3 receptor. Docking studies performed on compounds **28** and **56** revealed that both possibly interact with the orthosteric binding site on the M_5 receptor, which is consistent with the current results from the [3 H]NMS binding assay, indicating an orthosteric mechanism of action for these new analogues. We are building and validating homology

models for the other four mAChR subtypes, and these will be used for virtual library screening. The predictability of these models regarding mAChR subtype selectivity remains to be tested.

■ EXPERIMENTAL SECTION

Chemistry. All purchased reagents and solvents were used without further purification unless otherwise noted. All reactions sensitive to air and/or moisture were carried out under argon atmosphere in oven-dried glassware. Flash column chromatography was carried out using 32–63 μm , 60 Å (230–400 mesh) silica gel. Analytical thin layer chromatography was carried out on glass plates precoated with 250 μm silica gel 60 F₂₅₄. NMR spectra were recorded in CDCl_3 on a Varian 300 or 500 MHz spectrometer, and chemical shifts are reported in ppm relative to tetramethylsilane as the internal standard. Coupling constants are reported in hertz (Hz). Mass spectra were recorded on a JEOL JMS-700T MStation. GC–mass spectra were recorded on an Agilent 6890 GC incorporating an Agilent 7683 autosampler and an Agilent 5973 MSD. Elemental analyses were carried out on a COSTECH elemental combustion system and are within $\pm 0.4\%$ of theory. All final compounds for biological testing were prepared as salts in $\geq 95\%$ purity, in accord with results from combustion analysis. A detailed description of synthetic methodologies as well as analytical and spectroscopic data for all described compounds is included in the Supporting Information.

Binding Assay. Analogue binding affinities for the five mAChR subtypes were determined in assays evaluating inhibition of [^3H]NMS binding to membranes from CHO-K1 cells expressing one of the recombinant hM₁–hM₅ mAChRs. The CHO-K1 cell lines expressing the five subtypes of muscarinic receptors were obtained as a gift from Dr. Tom Bonner of National Institute of Mental Health (NIMH). Cells were grown at 37 °C with 5% CO₂ in Dulbecco's modified Eagle's medium (DMEM) supplemented with 10% fetal bovine serum, 4 mM glutamine, 50 ng/mL Geneticin G418 and 1% Pen–Strep. Cells were harvested at 70–90% confluency. To obtain cell membranes, cells were scraped into ice cold 50 mM Tris-HCl (pH 7.4), sonicated for 30 s, and centrifuged (48000g for 30 min). Pellets were resuspended in 1.5 mL of ice-cold 50 mM Tris-HCl buffer, sonicated for 30 s, and stored at –80 °C until assay. Assays were performed using 96-well plates. Membrane aliquots (100 μL) containing 10–40 μg of protein were added to wells containing 1 nM to 100 μM of test compound (25 μL), 0.3 nM [^3H]NMS (25 μL , scopolamine methyl chloride [*N*-methyl-3H], specific activity 82 Ci/mmol; Perkin-Elmer/NEN, Boston, MA), and buffer (50 mM Tris-HCl, pH 7.4, 125 μL) for a total volume of 250 μL . Atropine (1 mM) was used to determine nonspecific binding. Samples were incubated for 120 min at 25 °C with constant agitation. Reactions were terminated by rapid filtration onto GF/B filters using a Filtermate harvester (PerkinElmer Life and Analytical Sciences, Boston, MA). Samples were washed three times with 350 μL of ice-cold 50 mM Tris-HCl buffer and dried for 60 min at 50 °C. Subsequently, 40 μL of MicroScint 20 (PerkinElmer Life and Analytical Sciences, Waltham, MA) was added to each well and radioactivity bound determined using liquid scintillation spectrometry. IC₅₀ values were obtained and K_i values calculated using the equation of Cheng and Prusoff.⁴⁵

Inhibition of Oxotremorine-Evoked [^3H]DA Release Assay. Assays were performed according to previously published methods^{46,47} with minor modifications. Striata were dissected and coronal slices (500 μm , 4–6 mg) obtained with a McIlwain chopper. Slices were incubated for 30 min in Krebs' buffer (in mM: 108 NaCl, 4.7 KCl, 1.2 MgCl₂, 1 NaH₂PO₄, 1.3 CaCl₂, 11.1 glucose, 25 NaHCO₃, 0.11 L-ascorbic acid, and 0.004 disodium EDTA, pH 7.4, saturated with 95% O₂/5% CO₂) in a metabolic shaker at 34 °C. Slices were incubated with 0.1 μM [^3H]DA during the latter 30 min of a 60 min incubation period. Each slice was transferred to a superfusion chamber and superfused (0.6 mL/min at 34 °C) for 60 min with Krebs' buffer containing nomifensine (10 μM) and pargyline (10 μM) to inhibit reuptake and prevent metabolism, respectively, ensuring that [^3H]-overflow primarily represents [^3H]DA rather than [^3H]metabolites.⁴⁷

Sample collection began after 60 min of superfusion, when the rate of release was stable. Consecutive 4 min (2.4 mL) samples were collected to determine basal [^3H]outflow. Superfusion continued in the absence or presence of a range of analogue concentrations (0.1 nM to 1 mM) for 40 min, followed by 40 min with oxotremorine (100 μM) added to the superfusion buffer. Radioactivity in slices and superfusate samples were determined via liquid scintillation spectroscopy. Data were analyzed by weighted least-squares regression analysis of the sigmoidal concentration–effect curves to obtain IC₅₀ values.

Homology Modeling and Molecular Docking. The homology model of human M₅ mAChR was built based on the X-ray crystal structure of rat M₃ mAChR (PDB entry of 4DAJ at 3.4 Å resolution, A chain)⁴⁴ by using the Protein Modeling module of Discovery Studio (version 2.5.5, Accelrys, Inc., San Diego, CA). The model of human M₅ mAChR structure was constructed and refined in a very similar manner as in our previous study,⁴⁸ i.e., the best sequence alignment was selected based on both the alignment score and the reciprocal positions of the conserved residues among all mAChR subtypes. The coordinates of the conserved regions were directly transformed from the template structure, while the nonconserved residues were mutated from the template to the corresponding ones in M₅ mAChR. Structural optimization and energy minimization for the M₅ mAChR structure were performed using the Amber 11 program suite. The convergence criterion for the energy minimization was set to 0.001 kcal mol^{–1} Å^{–1}. On the basis of the optimized M₅ mAChR structure, the binding mode of the receptor with two lead compounds **28** and **56** was explored through molecular docking using the AutoDock 3.0.5 program.⁴⁸ This molecular docking approach was similar to that described in our previous study.⁴⁹ A reasonable binding structure of M₅ mAChR in complex with either compound **28** or **56** was obtained after energy minimization on each complex structure.

■ ASSOCIATED CONTENT

Supporting Information

Synthetic procedures and analytical data of all compounds prepared. This material is available free of charge via the Internet at <http://pubs.acs.org>.

■ AUTHOR INFORMATION

Corresponding Author

*Phone: 501-526-6787. Fax: 501-526-5945. E-mail: gzheng@uams.edu.

Notes

The authors declare no competing financial interest.

■ ACKNOWLEDGMENTS

This work was supported financially by a Pilot Project Grant from Center for Drug Abuse Research Translation at the University of Kentucky (Grant DA05312) and grants from National Institute of Drug Abuse, National Institutes of Health (Grants DA025948, DA030667, and TR000117).

■ ABBREVIATIONS USED

VTA, ventral tegmental area; NMS, *N*-methylscopolamine; CHO, Chinese hamster ovary; TM, transmembrane; EL, extracellular loop

■ REFERENCES

- (1) Caulfield, M. P. Muscarinic receptors—characterization, coupling and function. *Pharmacol. Ther.* **1993**, *58*, 319–379.
- (2) Caulfield, M. P.; Birdsall, N. J. International Union of Pharmacology. XVII. Classification of muscarinic acetylcholine receptors. *Pharmacol. Rev.* **1998**, *50*, 279–290.
- (3) Wess, J. Muscarinic acetylcholine receptor knockout mice: novel phenotypes and clinical implications. *Annu. Rev. Pharmacol. Toxicol.* **2004**, *44*, 423–450.

- (4) Wess, J.; Eglen, R. M.; Gautam, D. Muscarinic acetylcholine receptors: mutant mice provide new insights for drug development. *Nat. Rev. Drug Discovery* **2007**, *6*, 721–733.
- (5) Bonner, T. I.; Young, A. C.; Brann, M. R.; Buckley, N. J. Cloning and expression of the human and rat M₅ muscarinic acetylcholine-receptor genes. *Neuron* **1988**, *1*, 403–410.
- (6) Raffa, R. B. The M₅ muscarinic receptor as possible target for treatment of drug abuse. *J. Clin. Pharm. Ther.* **2009**, *34*, 623–629.
- (7) Di Chiara, G.; Imperato, A. Drugs abused by humans preferentially increase synaptic dopamine concentrations in the mesolimbic system of freely moving rats. *Proc. Natl. Acad. Sci. U.S.A.* **1988**, *85*, 5274–5278.
- (8) Koob, G. F.; Swerdlow, N. R. The functional output of the mesolimbic dopamine system. *Ann. N.Y. Acad. Sci.* **1988**, *537*, 216–227.
- (9) Koob, G. F.; Nestler, E. J. The neurobiology of drug addiction. *J. Neuropsychiatry Clin. Neurosci.* **1997**, *9*, 482–497.
- (10) Cami, J.; Farre, M. Drug addiction. *N. Engl. J. Med.* **2003**, *349*, 975–986.
- (11) Vilaro, M. T.; Palacios, J. M.; Mengod, G. Localization of M₅ muscarinic receptor messenger-RNA in rat-brain examined by in situ hybridization histochemistry. *Neurosci. Lett.* **1990**, *114*, 154–159.
- (12) Yasuda, R. P.; Ciesla, W.; Flores, L. R.; Wall, S. J.; Li, M.; Satkus, S. A.; Weisstein, J. S.; Spagnola, B. V.; Wolfe, B. B. Development of antisera selective for M₄ and M₅ muscarinic cholinergic receptors—distribution of M₄ and M₅ receptors in rat-brain. *Mol. Pharmacol.* **1993**, *43*, 149–157.
- (13) Weiner, D. M.; Brann, M. R. Distribution of M₁–M₅ muscarinic receptor messenger-RNAs in rat-brain. *Trends Pharmacol. Sci.* **1989**, *115*–115.
- (14) Reeve, C. M.; FerrariDiLeo, G.; Flynn, D. D. The M₅ (m5) receptor subtype: fact or fiction? *Life Sci.* **1997**, *60*, 1105–1112.
- (15) Yeomans, J. S.; Takeuchi, J.; Baptista, M.; Flynn, D. D.; Lepik, K.; Nobrega, J.; Fulton, J.; Ralph, M. R. Brain-stimulation reward thresholds raised by an antisense oligonucleotide for the M₅ muscarinic receptor infused near dopamine cells. *J. Neurosci.* **2000**, *20*, 8861–8867.
- (16) Miller, A. D.; Blaha, C. D. Midbrain muscarinic receptor mechanisms underlying regulation of mesoaccumbens and nigrostriatal dopaminergic transmission in the rat. *Eur. J. Neurosci.* **2005**, *21*, 1837–1846.
- (17) Lester, D. B.; Miller, A. D.; Blaha, C. D. Muscarinic receptor blockade in the ventral tegmental area attenuates cocaine enhancement of laterodorsal tegmentum stimulation-evoked accumbens dopamine efflux in the mouse. *Synapse* **2010**, *64*, 216–223.
- (18) Yamada, M.; Lamping, K. G.; Duttaroy, A.; Zhang, W. L.; Cui, Y. H.; Bymaster, F. P.; McKinzie, D. L.; Felder, C. C.; Deng, C. X.; Faraci, F. M.; Wess, J. Cholinergic dilation of cerebral blood vessels is abolished in M₅ muscarinic acetylcholine receptor knockout mice. *Proc. Natl. Acad. Sci. U.S.A.* **2001**, *98*, 14096–14101.
- (19) Basile, A. S.; Fedorova, I.; Zapata, A.; Liu, X.; Shippenberg, T.; Duttaroy, A.; Yamada, M.; Wess, J. Deletion of the M₅ muscarinic acetylcholine receptor attenuates morphine reinforcement and withdrawal but not morphine analgesia. *Proc. Natl. Acad. Sci. U.S.A.* **2002**, *99*, 11452–11457.
- (20) Fink-Jensen, A.; Sorensen, L.; Bay-Richter, C.; Frikke-Schmidt, H.; Wess, J.; Woldbye, D. P.; Wortwein, G. Involvement of the M₅ muscarinic receptor in cocaine and amphetamine induced behaviour: studies in M₅ knockout mice backcrossed to the C57BL/6NTac strain. *Schizophr. Res.* **2006**, *81*, 301–302.
- (21) Thomsen, M.; Woldbye, D. P. D.; Wortwein, G.; Fink-Jensen, A.; Wess, J.; Caine, S. B. Reduced cocaine self-administration in muscarinic M-5 acetylcholine receptor-deficient mice. *J. Neurosci.* **2005**, *25*, 8141–8149.
- (22) Rezayof, A.; Nazari-Serenjeh, F.; Zarrindast, M. R.; Sepehri, H.; Delphi, L. Morphine-induced place preference: involvement of cholinergic receptors of the ventral tegmental area. *Eur. J. Pharmacol.* **2007**, *562*, 92–102.
- (23) Yamada, M.; Basile, A. S.; Fedorova, I.; Zhang, W. L.; Duttaroy, A.; Cui, Y. H.; Lamping, K. G.; Faraci, F. M.; Deng, C. X.; Wess, J. Novel insights into M-5 muscarinic acetylcholine receptor function by the use of gene targeting technology. *Life Sci.* **2003**, *74*, 345–353.
- (24) Bridges, T. M.; Marlo, J. E.; Niswender, C. M.; Jones, C. K.; Jadhav, S. B.; Gentry, P. R.; Plumley, H. C.; Weaver, C. D.; Conn, P. J.; Lindsley, C. W. Discovery of the first highly M₅-preferring muscarinic acetylcholine receptor ligand, an M₅ positive allosteric modulator derived from a series of 5-trifluoromethoxy N-benzyl isatins. *J. Med. Chem.* **2009**, *52*, 3445–3448.
- (25) Bridges, T. M.; Kennedy, J. P.; Cho, H. P.; Breininger, M. L.; Gentry, P. R.; Hopkins, C. R.; Conn, P. J.; Lindsley, C. W. Chemical lead optimization of a pan G(q) mAChR M-1, M-3, M-5 positive allosteric modulator (PAM) lead. Part I: Development of the first highly selective M-5 PAM. *Bioorg. Med. Chem. Lett.* **2010**, *20*, 558–562.
- (26) Bridges, T. M.; Kennedy, J. P.; Hopkins, C. R.; Conn, P. J.; Lindsley, C. W. Heterobiaryl and heterobiaryl ether derived M₅ positive allosteric modulators. *Bioorg. Med. Chem. Lett.* **2010**, *20*, 5617–5622.
- (27) Liu, J.; Schoneberg, T.; van Rhee, M.; Wess, J. Mutational analysis of the relative orientation of transmembrane helices I and VII in G protein-coupled receptors. *J. Biol. Chem.* **1995**, *270*, 19532–19539.
- (28) Bohme, T. M.; Keim, C.; Dannhardt, G.; Mutschler, E.; Lambrecht, G. Design and pharmacology of quinuclidine derivatives as M₂-selective muscarinic receptor ligands. *Bioorg. Med. Chem. Lett.* **2001**, *11*, 1241–1243.
- (29) Bohme, T. M.; Augelli-Szafran, C. E.; Hallak, H.; Pugsley, T.; Serpa, K.; Schwarz, R. D. Synthesis and pharmacology of benzoxazines as highly selective antagonists at M(4) muscarinic receptors. *J. Med. Chem.* **2002**, *45*, 3094–3102.
- (30) Choppin, A.; Stepan, G. J.; Loury, D. N.; Watson, N.; Eglen, R. M. Characterization of the muscarinic receptor in isolated uterus of sham operated and ovariectomized rats. *Br. J. Pharmacol.* **1999**, *127*, 1551–1558.
- (31) Wang, Y.; Chackalamannil, S.; Hu, Z.; Greenlee, W. J.; Clader, J.; Boyle, C. D.; Kaminski, J. J.; Billard, W.; Binch, H., 3rd; Crosby, G.; Ruperto, V.; Duffy, R. A.; Cohen-Williams, M.; Coffin, V. L.; Cox, K. A.; Grotz, D. E.; Lachowicz, J. E. Improving the oral efficacy of CNS drug candidates: discovery of highly orally efficacious piperidinyl piperidine M₂ muscarinic receptor antagonists. *J. Med. Chem.* **2002**, *45*, 5415–5418.
- (32) Sagara, Y.; Sagara, T.; Uchiyama, M.; Otsuki, S.; Kimura, T.; Fujikawa, T.; Noguchi, K.; Ohtake, N. Identification of a novel 4-aminomethylpiperidine class of M₃ muscarinic receptor antagonists and structural insight into their M₃ selectivity. *J. Med. Chem.* **2006**, *49*, 5653–5663.
- (33) Augelli-Szafran, C. E.; Blankley, C. J.; Jaen, J. C.; Moreland, D. W.; Nelson, C. B.; Penrose-Yi, J. R.; Schwarz, R. D.; Thomas, A. J. Identification and characterization of m1 selective muscarinic receptor antagonists. *J. Med. Chem.* **1999**, *42*, 356–363.
- (34) Solymar, M. F., E.; Fulop, F. Enzyme-catalyzed kinetic resolution of piperidine hydroxy esters. *Tetrahedron: Asymmetry* **2004**, *15*, 3281–3287.
- (35) Inokuchi, E.; Narumi, T.; Niida, A.; Kobayashi, K.; Tomita, K.; Oishi, S.; Ohno, H.; Fujii, N. Efficient synthesis of trifluoromethyl and related trisubstituted alkene dipeptide isosteres by palladium-catalyzed carbonylation of amino acid derived allylic carbonates. *J. Org. Chem.* **2008**, *73*, 3942–3945.
- (36) Anagnostaras, S. G.; Murphy, G. G.; Hamilton, S. E.; Mitchell, S. L.; Rahnema, N. P.; Nathanson, N. M.; Silva, A. J. Selective cognitive dysfunction in acetylcholine M1 muscarinic receptor mutant mice. *Nat. Neurosci.* **2003**, *6*, 51–58.
- (37) Gerber, D. J.; Sotnikova, T. D.; Gainetdinov, R. R.; Huang, S. Y.; Caron, M. G.; Tonegawa, S. Hyperactivity, elevated dopaminergic transmission, and response to amphetamine in M₁ muscarinic acetylcholine receptor-deficient mice. *Proc. Natl. Acad. Sci. U.S.A.* **2001**, *98*, 15312–15317.

- (38) Naito, R.; Yonetoku, Y.; Okamoto, Y.; Toyoshima, A.; Ikeda, K.; Takeuchi, M. Synthesis and antimuscarinic properties of quinuclidin-3-yl 1,2,3,4-tetrahydroisoquinoline-2-carboxylate derivatives as novel muscarinic receptor antagonists. *J. Med. Chem.* **2005**, *48*, 6597–6606.
- (39) Choppin, A.; Eglen, R. M.; Hegde, S. S. Pharmacological characterization of muscarinic receptors in rabbit isolated iris sphincter muscle and urinary bladder smooth muscle. *Br. J. Pharmacol.* **1998**, *124*, 883–888.
- (40) McCombie, S. W.; Lin, S. I.; Tagat, J. R.; Nazareno, D.; Vice, S.; Ford, J.; Asberom, T.; Leone, D.; Kozlowski, J. A.; Zhou, G.; Ruperto, V. B.; Duffy, R. A.; Lachowicz, J. E. Synthesis and structure–activity relationships of M(2)-selective muscarinic receptor ligands in the 1-[4-(4-arylsulfonyl)-phenylmethyl]-4-(4-piperidinyl)-piperazine family. *Bioorg. Med. Chem. Lett.* **2002**, *12*, 795–798.
- (41) Watson, N.; Daniels, D. V.; Ford, A. P. D. W.; Eglen, R. M.; Hegde, S. S. Comparative pharmacology of human muscarinic M₃ and M₅ cholinergic receptors expressed in Chinese hamster ovary (CHO) cells. *Br. J. Pharmacol.* **1998**, *123*, U153–U153.
- (42) Pulido-Rios, M. T.; Steinfeld, T.; Armstrong, S.; Watson, N.; Choppin, A.; Eglen, R.; Hegde, S. S. In vitro isolated tissue functional muscarinic receptor assays. *Curr. Protoc. Pharmacol.* **2010**, *48*, 4.15.1–4.15.29.
- (43) Zhang, W.; Yamada, M.; Gomeza, J.; Basile, A. S.; Wess, J. Multiple muscarinic acetylcholine receptor subtypes modulate striatal dopamine release, as studied with M₁–M₅ muscarinic receptor knockout mice. *J. Neurosci.* **2002**, *22*, 6347–6352.
- (44) Kruse, A. C.; Hu, J.; Pan, A. C.; Arlow, D. H.; Rosenbaum, D. M.; Rosemond, E.; Green, H. F.; Liu, T.; Chae, P. S.; Dror, R. O.; Shaw, D. E.; Weis, W. I.; Wess, J.; Kobilka, B. K. Structure and dynamics of the M3 muscarinic acetylcholine receptor. *Nature* **2012**, *482*, 552–556.
- (45) Cheng, Y.; Prusoff, W. H. Relationship between the inhibition constant (K_i) and the concentration of inhibitor which causes 50% inhibition (I_{50}) of an enzymatic reaction. *Biochem. Pharmacol.* **1973**, *22*, 3099–3108.
- (46) Dwoskin, L. P.; Zahniser, N. R. Robust modulation of [³H]dopamine release from rat striatal slices by D-2 dopamine receptors. *J. Pharmacol. Exp. Ther.* **1986**, *239*, 442–453.
- (47) Zumstein, A.; Karduck, W.; Starke, K. Pathways of dopamine metabolism in the rabbit caudate nucleus in vitro. *Naunyn-Schmiedeberg's Arch. Pharmacol.* **1981**, *316*, 205–217.
- (48) Huang, X.; Zheng, G.; Zhan, C. G. Microscopic binding of M₅ muscarinic acetylcholine receptor with antagonists by homology modeling, molecular docking, and molecular dynamics simulation. *J. Phys. Chem. B* **2012**, *116*, 532–541.
- (49) Morris, G. M. G.; D. S.; Halliday, R. S.; Huey, R.; Hart, W. E.; Belew, R. K.; Olson, A. J. Automated docking using a Lamarckian genetic algorithm and empirical binding free energy function. *J. Comput. Chem.* **1998**, *19*, 1639–1662.